

BAYESIAN STRUCTURED SPARSITY FROM GAUSSIAN FIELDS

BY BARBARA E. ENGELHARDT AND RYAN P. ADAMS

Duke University and Harvard University

Substantial research on structured sparsity has contributed to analysis of many different applications. However, there have been few Bayesian procedures among this work. Here, we develop a Bayesian model for structured sparsity that uses a Gaussian process (GP) to share parameters of the sparsity-inducing prior in proportion to feature similarity as defined by an arbitrary positive definite kernel. For linear regression, this sparsity-inducing prior on regression coefficients is a relaxation of the canonical spike-and-slab prior that flattens the mixture model into a scale mixture of normals. This prior retains the explicit posterior probability on inclusion parameters—now with GP probit prior distributions—but enables tractable computation via elliptical slice sampling for the latent Gaussian field. We motivate development of this prior using the genomic application of association mapping, or identifying genetic variants associated with a continuous trait. Our Bayesian structured sparsity model produced sparse results with substantially improved sensitivity and precision relative to comparable methods. Through simulations, we show that three properties are key to this improvement: i) modeling structure in the covariates, ii) significance testing using the posterior probabilities of inclusion, and iii) model averaging. We present results from applying this model to a large genomic dataset to demonstrate computational tractability.

1. Introduction and Motivation. Sparsity is an important tool in applied statistics from three perspectives. First, in the settings where there are many more features than samples (so-called $p \gg n$ problems), employing a sparsity-inducing prior, or penalty term, has proven to be effective for regularization. For regression, the likelihood-maximizing parameters in the unregularized $p \gg n$ setting correspond to a continuum of solutions in a high-dimensional linear subspace. Many of these solutions will result in *overfitting*, in which the samples are well-captured by the parameters, but the model generalizes poorly for out-of-sample data. Overfitting is typically avoided by penalizing parameters, and in the Bayesian setting this corresponds to specifying a prior for the coefficients. In high dimensional problems, penalties that remove features by setting their contributions to 0 are ideal: rather than choosing the likelihood-maximizing parameters with the smallest Euclidean norm, overfitting may be overcome through *model selection*, or choosing feature set with the smallest number of elements. Model selection is performed for penalized regression by minimizing the ℓ_0 norm of the feature inclusion parameters. In practice, however, this is an exponentially large search space with 2^p possible solutions; convex relaxations provide popular and effective approximate objectives and enable computational tractability. Continuous Bayesian sparsity-inducing priors, such as the double-exponential (Hans, 2009) and the horseshoe (Carvalho et al., 2009), as well as explicit penalization approaches such as ℓ_1 (Lasso) (Tibshirani, 1996) and elastic net (Zou and Hastie, 2005), have been used effectively for such relaxation. Mapping these sparse feature parameters in the relaxed space back to the corners of a p -hypercube, in order to determine which features are included and which are excluded, must be performed thoughtfully, however.

Second, sparse priors often enable computational tractability by explicitly modeling a lower di-

mensional feature space (Tropp and Wright, 2010). Such computational savings have often been difficult to realize in practice; for example, the LARS algorithm for ℓ_1 regularized regression considers all features at each iteration (Efron and Hastie, 2004). One explanation for this behavior is that, in general, these methods were not optimized for the $p \gg n$ setting. Here we take advantage of sparsity to improve tractability in parameter estimation.

Third, sparsity, and model selection more generally, are crucial to the scientific goal of discovering which features are useful for our statistical task and which may be safely ignored (O’Hara and Sillanpää, 2009; Breiman, 2001). In problems across the sciences and beyond, estimating the relative contribution of each feature is often less important than estimating whether or not a feature contributes at all (Petretto et al., 2010). The downstream value of selecting a small subset of features is in creating a small number of testable hypotheses from which we can generalize scientific mechanisms (Efron, 2008). Occam’s Razor motivates the ℓ_0 penalty; conversely, estimating a contribution from every feature contradicts a simple explanation and, downstream, produces a more complex hypothesis to experimentally validate and to generalize across correlated scientific samples. The approach of model selection using some approximation to the ℓ_0 penalty has other downstream benefits as well. When the inclusion of a specific feature is modeled explicitly, so that the posterior probability of inclusion is estimated, we decouple the estimation of the effect size and the inclusion of the feature (Bottolo et al., 2011). This has the effect of removing the *Zero Assumption* (ZA) from the statistical test, which is the assumption that coefficients with effects near zero are null associations and should be excluded (Efron, 2008); the ZA is often false for a specific application, as truly alternative associations often have effect sizes near zero. Separately modeling signals and noise using a hierarchical model leads to more natural tests for association directly on the inclusion variable, and improves statistical power to detect associated predictors with small effects (Polson and Scott, 2010).

We examine the development of a Bayesian structured sparse prior within a linear regression framework. Let $\mathbf{y} \in \mathbb{R}^n$ be the continuous scalar responses for n samples. Let \mathbf{X} be an $n \times p$ matrix of predictors. We will use a linear regression model with independent Gaussian noise:

$$\mathbf{y} | \mathbf{X}, \boldsymbol{\beta}, \nu \sim \mathcal{N}(\mathbf{X}\boldsymbol{\beta}, \nu^{-1}\mathbb{I}_n),$$

where $\boldsymbol{\beta} \in \mathbb{R}^p$ is the vector of coefficients, $\nu > 0$ is the precision of the residual, and \mathbb{I}_n is the $n \times n$ identity matrix. The coefficients $\boldsymbol{\beta}$ are often referred to as *effect sizes*, because each β_j captures the slope of the linear effect of predictor j on the continuous response (Kendziorski et al., 2006; Stephens and Balding, 2009).

1.1. Bayesian approaches to sparsity. Bayesian sparsity uses a prior distribution for model selection to encourage a model to incorporate as few features as possible. A sparse prior on regression coefficients creates an *a priori* preference for $\boldsymbol{\beta}$ to be nonzero for only a subset of the predictors. In the absence of a detectable effect on the conditional probability of \mathbf{y} , a sparsity-inducing prior will encourage the β_j coefficient corresponding to predictor j to be 0, indicating no linear association between predictor j and the response, and excluding predictor j from the model. Parameter estimation in sparse Bayesian regression is performed by examining the posterior distribution on the β_j coefficients.

The canonical Bayesian sparsity-inducing prior is the spike-and-slab prior (Mitchell and Beauchamp, 1988; George and McCulloch, 1993). This *two-groups* prior introduces sparsity into the model via latent binary variables for each predictor that capture whether that predictor is modeled as noise or signal. That is, each dimension of $\boldsymbol{\beta}$ is taken to be a mixture of a Dirac delta function at zero (a *spike*, which assigns positive probability to the event that predictor j has exactly zero effect

on the response) and a continuous density function on \mathbb{R} (a *slab*, which regularizes the included predictor, allowing a wide range of possible contributions). The spike-and-slab formulation is

$$(1) \quad \beta_j | \omega, \tau \sim \omega \delta(\beta_j) + (1 - \omega) \mathcal{N}(\beta_j | 0, \tau^2),$$

where we are modeling the “slab” as a zero-mean Gaussian with variance τ^2 . The mixing parameter $\omega \in [0, 1]$ determines the expected proportion of sparse (excluded) components. This spike-and-slab prior is an elegant and direct approach to sparsity, in line with ℓ_0 regularization: it results in posterior hypotheses that directly quantify whether or not a particular predictor is relevant to the response. These hypotheses are explicitly represented as latent inclusion variables $z_j = \{0, 1\}$, which indicate whether predictor j is included or excluded from the model. When $z_j = 0$, the corresponding β_j is distributed according to a point mass at zero and when $z_j = 1$, β_j is marginally Gaussian. Thus, we may interpret the posterior probability of z_j as the probability that predictor j is included in the model, while the estimated effect size of predictor j (conditioned on the event $z_j = 1$) is modeled separately in β_j . There are a number of variations on this version of the spike-and-slab prior, all of which, to our knowledge, include an indicator variable that captures the inclusion of predictor j (Smith and Kohn, 1996; Ishwaran and Rao, 2005; Guan and Stephens, 2011). This elegant interpretation motivates the use of a two-groups prior for the regression framework when a sparse solution is desirable.

One of the challenges of the two-groups prior is the difficulty of managing the hypothesis space for the z_j variables, which has 2^p discrete configurations. The need for computational tractability has catalyzed the burgeoning field of continuous Bayesian sparsity-inducing priors; these priors encourage the removal of features from the model, but in a computationally tractable one-group framework (Polson and Scott, 2010). One continuous prior is the Laplacian, or double exponential, prior, the Bayesian analog to the Lasso (Tibshirani, 1996; Hans, 2009). Another approach, the Gaussian-inverse gamma prior, called the *automatic relevance determination* (ARD) prior in the machine learning literature (Tipping, 2001), induces sparsity via a scale mixture of Gaussians with an inverse gamma mixing measure on predictor-specific variance terms. This class of scale mixtures corresponds to the Student’s t-distribution when integrating over the predictor-specific variance parameters, and, when the degrees-of-freedom parameter $\nu = 1$, it reduces to the Cauchy distribution; both of these have been suggested as approaches to one-group Bayesian sparsity (Polson and Scott, 2010). Other more recent continuous sparsity-inducing priors include the *horseshoe* (Carvalho et al., 2009, 2010), the generalized double Pareto (Armagan et al., 2011a), the three parameter beta (Armagan et al., 2011b), and the Dirichlet Laplace prior (Bhattacharya et al., 2012). These continuous priors differentially modulate shrinkage effects for large and small signals while avoiding the computational challenges associated with discrete sparsity models. In particular, each of these one-group continuous priors has substantial density around zero, shrinking noise to zero, and heavy, sub-exponential tails, allowing large signals to remain intact, without explicitly parameterizing predictor inclusion (Mohamed et al., 2011). For a review of Bayesian sparsity-inducing priors, see Polson and Scott (2010).

While one-group priors are appealing for computational reasons as continuous relaxations of discrete model-selection problems, they obfuscate the core statistical questions surrounding estimates and tests of inclusion (Richardson et al., 2010). The posterior distribution of parameter β_j captures the marginal effect size of the predictor j on the response, and, in the context of model selection, a zero-valued β_j excludes predictor j from the model. Under continuous one-group priors and practical likelihoods, however, $\beta_j = 0$ measure zero under the posterior. That is, none of the β_j variables will be exactly zero with positive probability. In practice, often a global threshold on the

estimated effect size is defined to determine model inclusion based on the estimated $\hat{\beta}_j$ variables. Using these posterior distributions to evaluate model inclusion is not statistically well-motivated with finite samples: features with small effect sizes may be excluded because the resulting bimodal distribution of significant effect sizes explicitly excludes predictors with estimated effects in a region around zero. We prefer to avoid this zero assumption and instead use a two-groups prior.

1.2. Structured sparsity. One assumption of the generic Bayesian regression model is that the predictors are uncorrelated. In practical applications, this assumption is frequently violated (Breiman, 2001). The problem of correlated or structured predictors has been studied extensively in the classic statistical literature (Jacob et al., 2009; Liu et al., 2008; Chen et al., 2012; Jenatton et al., 2011a; Kim and Xing, 2009), and a number of methods that explicitly represent structure in the predictors have been introduced for regression. Group Lasso (Yuan and Lin, 2005) uses a given disjoint group structure and jointly penalizes the predictors group-wise using a Euclidean norm. This model induces sparsity at the group level: the penalty will either remove all features within a group or impose an ℓ_2 penalty uniformly across features within a group. This creates a *dense-within-groups* structure, as groups of predictors included in the model will not be encouraged to have zero coefficients. The sparse group Lasso (Friedman et al., 2010) extended this idea by including an ℓ_1 penalty on the included groups' coefficients, creating a *sparse-within-groups* structure. A Bayesian group Lasso model has also been developed (Kyung et al., 2010), where sparsity is encouraged with a normal-gamma prior on the regression coefficients, and the group structure is encouraged by sharing the gamma-distributed variance parameter of the sparsity-inducing prior within a group. This prior will also have a dense-within-groups structure, as all included coefficients within a group will have a normal-gamma prior with shared parameters, which will not induce zeros within included groups.

Structured sparsity has proven to be useful in a wide variety of practical applications such as image denoising, topic modeling, and energy disaggregation (Kolter et al., 2010; Jenatton et al., 2011b). Despite its utility in applied statistics, few proposals have been made for Bayesian structured sparsity models; exceptions include Kyung et al. (2010) and Bottolo et al. (2011). This area of research is ripe for innovation, as the Bayesian paradigm allows us to incorporate structure naturally for heterogeneous data in a hierarchical model to improve task performance. Applied Bayesian statisticians in particular may find that a Bayesian structured sparse framework needs little tailoring to be customized to a specific application other than a careful definition of the domain-specific structure on the predictors, in contrast to the practical realities in the broader literature (Kim and Xing, 2009; Jenatton et al., 2011b).

In a Bayesian context, it is natural to impose structure through the prior probability of the sparse parameters, sharing local shrinkage priors between similar predictors (Kyung et al., 2010). Such hierarchical models are straightforward to describe, and the Bayesian formalism allows flexibility in the semantics of the structural representation. For example, a common theme among many structured sparsity methods, including group Lasso, Bayesian group Lasso, and tree Lasso (Kim, 2009), is that the structure among the predictors is defined as a discrete partition of feature space. This disjoint encoding of structure is not always possible, however, and many applications require a more general notion of similarity between predictors. A flexible Bayesian approach would enable application-driven “soft” measures of inclusion-relevant similarity. This representational flexibility comes at a computational cost, however, and such structured sparsity models must be designed with considerations for the trade-off between the complexity of the representation and inferential tractability.

In this paper, we describe a flexible Bayesian model for relaxed two-groups sparse regression

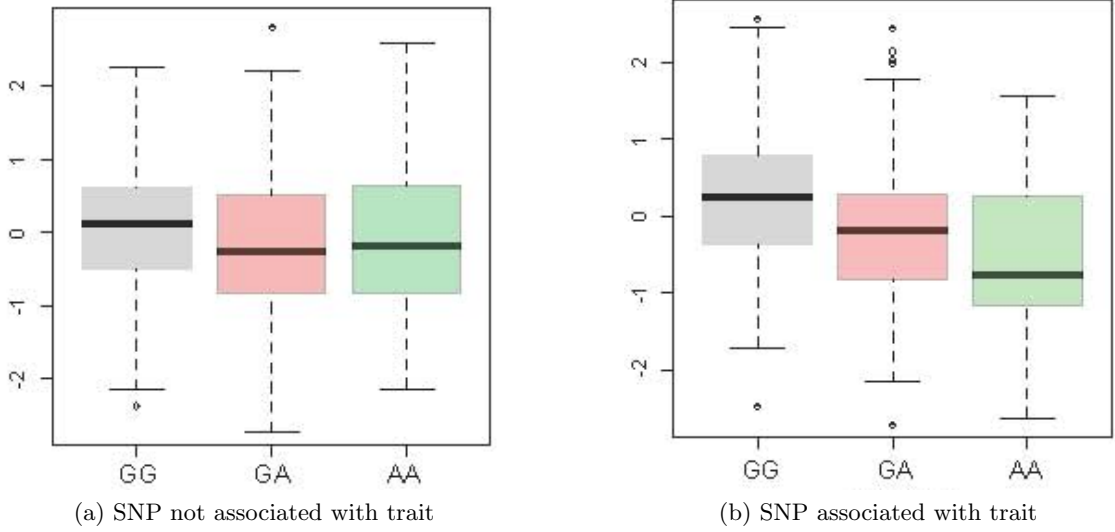


Fig 1: **Examples of an SNP-trait pair with no evidence of association, and a SNP-trait pair with evidence of association.** For both, x-axis is a single SNP; y-axis is a single quantitative trait.

that includes a positive definite matrix representing an arbitrary, continuous measure of similarity between all pairs of predictors. Despite considerable work on structured sparse models in the classical framework, we are not aware of substantial prior work on Bayesian structured sparse methods beyond those mentioned above. We ground our modeling approach with a specific motivating domain: the problem of associating genetic variants with quantitative traits, which we describe in the proceeding section. In addition to our general-purpose model, we describe a Markov chain Monte Carlo sampler for parameter estimation that enables the model to be applied to large numbers of predictors by exploiting the structure of the predictors to improve mixing. We examine the empirical performance of our approach by applying our model to simulated data based on the motivating example of identifying genetic variants associated with a quantitative trait. Finally, we describe the application of our model to identify genetic variants that regulate gene expression levels across 40 million genetic variants and more than 17,000 genes, and we compare results from our model to results from a univariate approach to association mapping.

2. Motivating application: associating genetic variants with quantitative traits. Bayesian structured sparsity for linear regression is well-motivated by the challenge of identifying genetic variants that are associated with a quantitative trait, such as expression levels of a gene. For this problem, $\mathbf{y} \in \mathbb{R}^n$ represents the quantitative trait measurement across n samples, and the predictors are single nucleotide polymorphisms (*SNPs*). We assume that each individual has two copies of each nucleotide and that there are exactly two possible *alleles*, or variants, for each SNP. SNPs are encoded as $X_{i,j} \in \{0, 1, 2\}$, which represent the number of copies of the minor (or less frequent) allele for individual $i \in 1, \dots, n$ at one SNP $j = 1, \dots, p$. The Bayesian testing problem is then to determine which of the SNPs are associated with a given continuous response, or quantitative trait; in other words, we wish to identify each SNP j where the true effect size on the trait, parameterized through the β_j coefficients, is non-zero (Figure 1).

The *de facto* approach to identifying genetic associations (called *association mapping*) is to

regress trait on SNPs for n individuals, and then examine the magnitude of the estimated linear coefficient $\hat{\beta}$ (Kendziorski et al., 2006). Testing for association is performed by computing p-values or Bayes factors that compare the likelihood given $\beta = 0$ (null hypothesis, no effect) versus $\beta \neq 0$ (alternative hypothesis, effect) (Stephens and Balding, 2009). Modeling and testing is often performed in a univariate way, i.e., for a single trait and p distinct SNPs, we will have p linear models and p separate tests, one for each SNP. Typically, the number of individuals, n , is in the range of 100 – 10,000, and the number of SNPs, p , is in the range 10,000 – 40,000,000. The additional caveat is, in current studies, there are often a large number of quantitative traits, as in our application below.

A few approaches have combined these univariate models into a single multivariate regression model, *multi-SNP association mapping*, by including all p SNPs as the predictors. Then a sparsity-inducing prior may be placed on the coefficient vector β in order to regularize appropriately in this $p \gg n$ regression with more predictors (SNPs) than samples. A sparse prior also matches our belief that a small subset of SNPs will have a measurable regulatory effect on a quantitative trait. Indeed, multi-SNP association mapping is an elegant example of an application of sparse models where the underlying signal is thought to be truly sparse, as opposed to the data being collected in such a way as to produce sparse signals (Tibshirani, 2014).

Sparse multivariate regression controls the combinatorial explosion of univariate approaches by assuming additive effects across SNPs. When nonadditive interactions among the SNPs are present—called *epistatic effects*—these additive models are useful approximations (Storey et al., 2005), as current methods to detect epistatic effects are infeasible due to a lack of statistical power. Many multi-SNP association studies use greedy approaches to sparse regression. Forward stepwise regression (FSR) (Brown et al., 2013; Stranger et al., 2012) is one greedy approach, with stopping criteria defined by model scores such as AIC or BIC (Schwarz, 1978). The model starts with zero included SNPs, and a SNP is included in the model if the model selection score improves maximally with respect all other excluded SNPs; the algorithm iterates, including a single SNP on each iteration, until none of the excluded SNPs improves the current score. Conditional analyses have been proposed (Lango Allen et al., 2010; Yang et al., 2012, 2010) that identify the most significant QTL association, and search for additional single or pairwise associations conditional on the associations identified thus far. Penalized regression, specifically Lasso, has also been used for multi-SNP association mapping (Hoggart et al., 2008; Wu et al., 2009).

Other model-based methods for detecting genetic associations in the additive setting have used a combination of sparse regression and model averaging (Brown et al., 2002). Model averaging protects against the substantial type I and type II errors that result from a non-robust point estimate of the independently associated SNPs. For example, if two SNPs are perfectly correlated, or in perfect LD, and only one is a causal SNP, a sparse method applied to the sample may select either one of these SNPs with similar frequency. In this case, there is insufficient information from which to determine the causal variant, and model averaging protects us from making the wrong choice. A recent approach used the Lasso, or ℓ_1 penalized regression, along with model averaging (Valdar et al., 2012) based on ideas from stability selection (Meinshausen and Peter, 2010). Bayesian model averaging has not often been applied to this problem for a number of reasons, one of which is that the LD structure of the SNPs slows down the mixing rate of sampling methods considerably. Exceptions include the MISA model (Wilson et al., 2010), which uses Bayesian model averaging to address the correlation in SNPs and also tests for association directly on the posterior probability of inclusion. A recent Bayesian multivariate approach not only included p SNPs but also q traits, developing a multi-trait regression model with a matrix response (Bottolo et al., 2011). This model

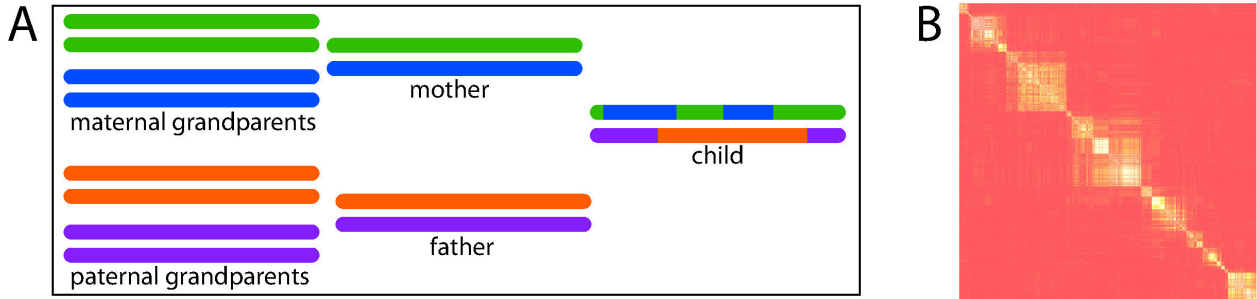


Fig 2: Recombination and linkage disequilibrium in the human genome. **(A)** A single chromosome from each grandparent recombines in the parents; neighboring loci in the child chromosome will have identical grandparent of origin, except across sites of recombination. **(B)** Heatmap of the absolute value Pearson's correlation among a thousand SNPs in a chromosomal region showing the block-like LD-structure in the genome.

used a sparse hierarchical prior on the coefficients and clever methods for parameter estimation in this high-dimensional space. Other Bayesian methods have used approximations to the spike-and-slab prior (Guan and Stephens, 2011), but not included structure on the predictors or model selection.

In this application there is substantial structure among the predictors. *Linkage disequilibrium* (LD) refers to the non-random assortment of genetic variants. When offspring inherit one complete set of chromosomes from each of their parents, each pair of chromosomes that a parent inherited from his parents *recombines* in a handful of positions, so that a child receives a combination of her grandparents' chromosomes for autosomal, or non sex-linked, chromosomes (Figure 2). But because of the relative infrequency of a recombination event, neighboring sites on a child's chromosome are likely to be inherited together from the same grandparent (Figure 2) (Fledel-Alon et al., 2011). Local, or *background*, LD tends to result in block-like correlation structure among SNPs on a chromosome (Figure 2) (Gabriel et al., 2002). The correlated groups of SNPs are neither well-defined nor mutually exclusive, and these correlations may exist across long genomic distances (Consortium et al., 2005).

In order to be useful in generating hypotheses for downstream experimental validation and for use in clinical research, the goal of association mapping—and *fine mapping* in particular—is to identify the *causal SNP* for a given trait, or the SNP that, if modified, would affect a change in that trait through biological machinery. The correlation structure between SNPs, however, means that the identity of the causal SNP is uncertain within the set of well correlated SNPs with a similar association significance. Current practice with univariate and hierarchical approaches select the SNP with the greatest significance, but the assumption of exactly zero or one associated SNPs does not match our understanding of genomic regulation (Stranger et al., 2012; Wood et al., 2011). This assumption dramatically oversimplifies the solution to the point of not producing robust, interpretable results (Maranville et al., 2011; Guan and Stephens, 2011; Mangravite et al., 2013). The biological scenario where multiple genetic loci affect a trait through independent mechanisms is called *allelic heterogeneity* (Wood et al., 2011). We take a sparse multivariate approach to test for all independently associated SNPs.

A further difficulty of this application is that, because we observe a subset of SNPs in our data, the causal SNP may be missing. *Tag SNPs* are correlated with a causal SNP and may confound the results: if there are multiple tag SNPs for an unobserved causal QTL, it is possible that they

split the effect of the causal QTL, appearing independently associated with the trait and acting as surrogate predictors in the association model.

3. A model for Bayesian structured sparsity. We now describe our prior for two-group sparse regression using a Gaussian field. We assume the data are n samples with p predictors $\{\mathbf{x}_i, y_i\}_{i=1}^n$, $\mathbf{x}_i \in \mathbb{R}^p$, and $y_i \in \mathbb{R}$. We will encode this response as an n -vector $\mathbf{y} \in \mathbb{R}^n$ and the predictors as a matrix $\mathbf{X} \in \mathbb{R}^{n \times p}$. The response variables are conditionally independent, given the predictors and three parameters:

$$(2) \quad \mathbf{y} | \mathbf{X}, \boldsymbol{\beta}, \beta_0, \nu \sim \mathcal{N}(\beta_0 \mathbf{1}_n + \mathbf{X}\boldsymbol{\beta}, \nu^{-1} \mathbb{I}_n),$$

where we have separated out the offset $\beta_0 \in \mathbb{R}$, $\mathbf{1}_n$ is a length- n column vector of ones, $\boldsymbol{\beta} \in \mathbb{R}^p$ is the vector of weights, and $\nu > 0$ is the residual precision. We place a (conjugate) gamma prior on the residual precision:

$$(3) \quad \nu \sim \text{Gam}(a_\nu, b_\nu).$$

For concreteness, we assume the following parameterization of the gamma distribution:

$$(4) \quad p(x | a, b) = \frac{b^a}{\Gamma(a)} x^{a-1} \exp\{-bx\}.$$

We place a zero-mean Gaussian prior on the offset:

$$(5) \quad \beta_0 \sim \mathcal{N}(0, (\lambda\nu)^{-1}).$$

It is useful to recall that the Dirac delta function can be interpreted as the limit of a zero-mean Gaussian distribution as the variance goes to zero. With this in mind, when conditioning on the latent spike-and-slab inclusion variables z_j (where $z_j = 0$ indicates exclusion through a “spike” and $\beta_j = 0$, and $z_j = 1$ indicates inclusion, and the associated β_j is drawn from the “slab”), we form a degenerate diagonal covariance matrix $\boldsymbol{\Gamma}$, where $\Gamma_{j,j} = z_j$, and write a single p -dimensional Gaussian prior that captures both included and excluded predictors:

$$(6) \quad \boldsymbol{\beta} | \nu, \lambda, \boldsymbol{\Gamma} \sim \mathcal{N}(\mathbf{0}, (\nu\lambda)^{-1} \boldsymbol{\Gamma}).$$

Here λ is an inverse squared global scale parameter for the regression weights, on which we place a gamma prior:

$$(7) \quad \lambda \sim \text{Gam}(a_\lambda, b_\lambda).$$

We follow Jeffreys ([Jeffreys, 1998](#); [Polson and Scott, 2010](#)) and scale the global shrinkage parameter λ by the residual precision ν .

3.1. Structure from a Gaussian field. We introduce structure into the sparsity pattern of $\boldsymbol{\beta}$ by replacing independent z_j —which in Eq. 1 would be Bernoulli with $P(z_j = 0) = \omega$ —with a probit link ([Bliss, 1935](#); [Albert and Chib, 1993](#)) driven by a latent Gaussian field

$$(8) \quad \boldsymbol{\gamma} \sim \mathcal{N}(\mathbf{0}, \boldsymbol{\Sigma}).$$

The diagonal $\Gamma_{j,j}$ is then determined by whether γ_j exceeds a threshold γ_0 , i.e., $\Gamma_{j,j} = \mathbb{1}(\gamma_j > \gamma_0)$. We assume that the positive definite covariance matrix $\boldsymbol{\Sigma}$ is known; this matrix is used to specify

the dependence structure for inclusion. We complete the hierarchical model by placing a Gaussian prior on the probit threshold γ_0 :

$$(9) \quad \gamma_0 \sim \mathcal{N}(\mu_\gamma, v_\gamma).$$

The marginal prior probability of inclusion of predictor j is computed directly via

$$(10) \quad P(\beta_j \neq 0) = 1 - \Phi\left(\frac{\gamma_0}{\Sigma_{j,j}}\right),$$

where $\Phi(\cdot)$ is the cumulative distribution function of the standard normal. Under the often reasonable restriction that Σ be a correlation matrix with ones on the diagonal, the expected number of included predictors is $p \cdot (1 - \Phi(\gamma_0))$. Conditioned on data, the posterior probability of $\Gamma_{j,j}$ is the posterior probability of inclusion (PPI) for the j^{th} predictor.

In Equation (8), the covariance matrix Σ may be the identity matrix, in which case this reduces to an unstructured Bayesian model of sparse regression of Eq. 1, with $\omega = \Phi(\gamma_0)$. This formulation also encompasses Bayesian (disjoint) group sparse regression when Σ has a block diagonal structure with constant non-negative values within each block. However, the advantage of this construction is the ability to include structure in the sparsity-inducing prior, and so Σ can be an arbitrary positive definite matrix. Of particular interest is the case where the matrix Σ captures the pairwise similarity between the predictors, i.e., the Gram matrix of a Mercer kernel. As with structured sparse regression models in the group Lasso and related literature, predictors that are similar will have correlated priors on the model exclusion parameters through the covariance matrix. This has the effect of smoothing the γ_j parameters for similar predictors using a Gaussian process (GP). GP structure has been considered before for probit regression models ([Girolami and Rogers, 2006](#)), but neither appear to have been used to induce (structured) sparsity.

3.2. Example: Structured Matrices for SNPs. The choice of kernel function requires some thought for any application. For the problem of association mapping, we considered a number of possible Mercer kernels that reflect the similarity between SNPs, including:

- *covariance*: $\Sigma^{cov} = X^T X$
- *absolute value Pearson's correlation*: $\Sigma_{j,k}^{cor} = \left| \frac{(X_j - \bar{X})^T (X_k - \bar{X})}{\sqrt{(X_j - \bar{X})^T (X_j - \bar{X})} \sqrt{(X_k - \bar{X})^T (X_k - \bar{X})}} \right|$, where \bar{X} is the empirical mean of each feature X_j across n samples.
- *mutual information*: Σ^{mi} , a positive definite kernel based on a generalization of a Fisher Kernel ([Seeger, 2000](#)).
- *centimorgan*: Σ^{cm} , a quantification of genetic linkage between two SNPs (empirically derived, e.g., ([Durbin et al., 2010](#))).

We found that the choice of kernel within this set made minimal difference in the simulation results, and for simplicity we chose the absolute value Pearson's correlation kernel for our results. In practice, we ensure that each of these matrices are positive definite by including a small regularization term on the diagonal.

Kernel functions are application specific; an arbitrary Mercer kernel may be designed for other applications. While our choice of kernel in this application is effective, it is a semantic approximation to our true definition of “similar” in the setting of association mapping. In particular, using this kernel it is difficult to discriminate independently functional, but correlated, SNPs from similarly functional, but correlated, SNPs. In other words, when two SNPs are well correlated, and we find that they both are associated with a gene via a univariate model, then two scenarios are possible: i)

conditioning on one of the SNPs in the same univariate model, the other SNP is no longer correlated with the gene (the SNPs are *similarly functional*), or ii) in this conditional framework, the other SNP remains associated with the gene levels (the SNPs are *independently functional*). Ideally, our kernel would indicate high similarity for correlated and similarly functional SNP pairs, but low similarity for correlated and independently functional SNP pairs. Current work is focused on using additional biological information, such as co-localized cis-regulatory elements (Brown et al., 2013) and evolutionary signatures (Rasmussen et al., 2014), to achieve this quantification of similarity and improve association mapping. This framework would also allow us to invert the problem to investigate, in an iterative way, evolutionary and genomic signatures of functional SNPs through evaluation of specific kernels in discovering these truly causal SNPs. Our Bayesian framework enables data-driven inference of the relevant similarity between predictors, referred to as *adaptive basis functions*, in which the kernel function is parameterized and those parameters are estimated via the inference process. While we did not estimate covariance parameters here, we expect this will be useful as the biological semantics of the kernels become more complex.

Another comment about the kernel function focuses on the possible concern that the data are used twice: once to estimate the Gram matrix and again during inference to estimate model parameters. Given copious available genomes, we suggest that the Gram matrix for this application be estimated using reference genomic data, ideally from the same population as the study data. Using reference data to estimate the Gram matrix is well motivated because, in general, we expect QTLs to replicate across studies (Brown et al., 2013). Thus, although there are caveats, a causal SNP in the study sample is likely to be causal in the reference sample, and, by this reasoning, similarities between SNPs should be meaningfully transferable.

4. Parameter estimation with MCMC. In many applications, the central quantities of interest are the marginal PPIs. In the context of genetic association studies, PPIs allow us to test for association of the SNP with a trait, which is the essential parameter for finding biologically functional genetic variants. These can be estimated via Markov chain Monte Carlo (MCMC) using posterior samples of γ and γ_0 . Of particular interest is the estimation of the posterior inclusion while marginalizing out the effect size captured by β . The degenerate Gaussian form of Eq. 6 makes it possible to perform this marginalization in closed form and view the posterior on γ and γ_0 through a regression marginal likelihood:

$$\begin{aligned}
p(\mathbf{y} | \mathbf{X}, \gamma, \gamma_0, \nu, \lambda) &= \int \int \mathcal{N}(\mathbf{y} | \beta_0 \mathbf{1}_n + \mathbf{X}\beta, \nu^{-1} \mathbb{I}_n) \mathcal{N}(\beta | \mathbf{0}, (\nu\lambda)^{-1} \mathbf{\Gamma}) \mathcal{N}(\beta_0 | 0, (\nu\lambda)^{-1}) d\beta d\beta_0 \\
&= \int \mathcal{N}(\mathbf{y} | \beta_0 \mathbf{1}_n, \nu^{-1} (\lambda^{-1} \mathbf{X}\mathbf{\Gamma}\mathbf{X}^\top + \mathbb{I}_n)) \mathcal{N}(\beta_0 | 0, (\nu\lambda)^{-1}) d\beta_0 \\
(11) \quad &= \mathcal{N}(\mathbf{y} | \mathbf{0}, \nu^{-1} (\lambda^{-1} (\mathbf{1}_n \mathbf{1}_n^\top + \mathbf{X}\mathbf{\Gamma}\mathbf{X}^\top) + \mathbb{I}_n))
\end{aligned}$$

In the Markov chain simulation, we update each of the parameters γ , γ_0 , λ , and ν in turn (Bottolo et al., 2011).

Updating γ . We use elliptical slice sampling (ESS), a rejection-free Markov chain Monte Carlo (MCMC), for defining and simulating transition operators on γ (Murray et al., 2010). ESS samples efficiently and robustly from latent Gaussian models when significant covariance structure is imposed by the prior, as in Gaussian processes and the present structured sparsity model. The conditional density on γ is the product of the likelihood in Eq. 11 and prior in Eq. 8. ESS generates random elliptical loci using the Gaussian prior and then searches along these loci to find acceptable points for slice sampling. When the data are weakly informative and the prior is strong, as is the

case here, the elliptical loci effectively capture the dependence between the variables and enable faster mixing. Here, using ESS for γ enables us to avoid directly sampling over the large discrete space of sparsity patterns that makes unstructured spike-and-slab computationally challenging. We also note that elliptical slice sampling requires no tuning parameters, unlike alternative procedures such as Metropolis–Hastings or Hamiltonian Monte Carlo, which may mix faster but are often difficult to tune and make robust.

Updating γ_0 and λ . The scalar γ_0 specifies the probit threshold and, conditioned on γ , it determines which entries on the diagonal of Γ are zero and which are one. The scalar parameter λ determines the scale of the “slab” portion of the weight prior. Neither of these conditional densities has a simple closed form, but they can each be efficiently sampled using the exponential-expansion slice sampling algorithm described in (Neal, 2003).

Updating ν . The scalar ν determines the precision of the residual Gaussian noise of the response variables. With the choice of a conjugate gamma prior distribution, the conditional posterior is also gamma:

$$(12) \quad p(\nu | \mathbf{y}, \mathbf{X}, \boldsymbol{\Gamma}, \lambda) \propto \mathcal{N}(\mathbf{y} | \mathbf{0}, \nu^{-1}(\lambda^{-1}(\mathbf{1}_n \mathbf{1}_n^\top + \mathbf{X} \boldsymbol{\Gamma} \mathbf{X}^\top) + \mathbb{I}_n)) \text{Gam}(\nu | a_\nu, b_\nu)$$

$$(13) \quad = \text{Gam}(\nu | a_\nu^{(n)}, b_\nu^{(n)})$$

$$(14) \quad a_\nu^{(n)} = a_\nu + \frac{N}{2}$$

$$(15) \quad b_\nu^{(n)} = b_\nu + \frac{1}{2} \mathbf{y}^\top (\lambda^{-1}(\mathbf{1}_n \mathbf{1}_n^\top + \mathbf{X} \boldsymbol{\Gamma} \mathbf{X}^\top) + \mathbb{I}_n)^{-1} \mathbf{y}.$$

5. Results. To evaluate our model, we first used simulated trait data with existing SNP data to compare methods where the complexity of the predictor relationships was real, but the truth was known. We compared our model against a number of other methods for association mapping using precision-recall curves. Then, using these same SNP data, we performed genome-wide association mapping with 16,424 quantitative traits, and compared the results from our method with results from univariate Bayesian association mapping. The genomic data, from the HapMap phase 3 project (Consortium et al., 2010), include 608 individuals that we imputed to give us 40 million SNPs per individual; a complete description of these data, including quality control and pre-processing performed, can be found in Stranger et al. (2012) and Brown et al. (2013).

5.1. Simulation Results. Using simulations, we evaluated the performance of our model in analyzing realistically complex genetic relationships, but with known ground truth. We simulated association data based on quantitative traits sampled from a linear model with real SNP data as the predictors. In particular, given publicly available SNP data, we first generated effect sizes for a small subset of randomly chosen SNPs. Next we generated a quantitative trait based on weighted linear combinations of those included SNPs.

Simulating data.. From the HapMap data, we selected 200 SNPs at random from all SNPs in one genetic locus, where loci were chosen from regions where we expect SNPs to be functional (see below). We then selected at random $q \in [2, 6]$ QTLs per trait chosen from these 200 SNPs Q . We generated weights β , representing the effect size, from a $\beta_j \sim \text{Be}(0.1, 0.1)$ distribution, and we rescaled β_j to lie between $(-1, 1)$. The rationale behind this simulation was to allow for effect sizes that were closer to 1 or -1 than to zero; this scenario will favor the methods that make the zero assumption over ours. After generating a quantitative trait from $y_i \sim \mathcal{N}(Q_i \beta, 1)$, we projected each

trait to the quantiles of a standard normal (i.e., *quantile normalized* them). We repeated this for 696 arbitrarily chosen genetic loci. We call these data *Sim1*.

A second simulation, *SimTag*, considers the possibility that a causal QTL may not be included in the set of SNPs, as may be the case with genotyping data. In this simulation, we quantified how often the methods incorrectly identify a *tag SNP*, or a SNP that is correlated with the causal SNP, when the causal SNP is missing. In order to generate these data, we used an identical procedure as for generating quantitative traits in Sim1, except we selected between 2 and 8 eQTLs (s) and chose some subset of those r to remove from the matrix Q from a set of $200 + r$ randomly chosen cis-SNPs, where $s - r > 0$. The subsequent steps—generating a trait using s eQTLs and quantile normalizing the trait across individuals—are identical to the steps in Sim1.

Methods for comparison. Our evaluations compared results from a number of different methods, some of which have been used for association mapping and others which are common methods for model selection. We ran Lasso regression fitted using Least Angle Regression (LARS), and identified the penalty term by selecting the point in the LARS path with the smallest Bayesian information criterion (BIC) score (Hoggart et al., 2008; Efron and Hastie, 2004; Schwarz, 1978). We ran forward stepwise regression (FSR), using the BIC score to determine when to stop adding predictors to the model (Brown et al., 2013). We ran Bayesian sparse regression with an ARD prior on the weights (ARD) (Tipping, 2001). We applied our model of Bayesian sparse regression with $\Sigma = \mathbb{I}_p$ (identity matrix for the covariance of the Gaussian field) to study our scale mixture representation of spike-and-slab regression without structure on the predictors (BSR). We used 500 iterations of burn-in for ESS and 1000 iterations for collection. We also ran our model of Bayesian structured sparse regression with Σ^{cor} to model the correlation structure of the predictors (BSSR) with the same number of ESS iterations as BSR. For BSSR, we also report results without model averaging by selecting the configuration of the inclusion parameters with the best posterior probability during sampling (MAPS).

We evaluated the results of applying our method to these simulated data using precision-recall (PR) curves. In our simulations, only the causal SNPs, or the SNPs selected in the simulation with a non-zero effect, were considered *truly alternative*; nearby SNPs that were well correlated (or perfectly correlated) with the causal SNP but had no simulated effect on the trait were considered to be *truly null* in order to compute the true positive rates (TPR) and false discovery rates (FDR) (Storey and Tibshirani, 2003). Results for FSR, Lasso, and ARD are determined by thresholding the estimated effect sizes $\hat{\beta}$; results from BSR, BSSR, and MAPS are determined by thresholding the estimated PPI.

Comparison on simulated data.. On Sim1, the comparative precision-recall curves show that BSSR performs well across most levels of precision, particularly at high precision, or, equivalently, low FDR (Figure 3). FSR appears uniformly to give the poorest performance; at a threshold of zero, the recall of FSR remains below 0.5. In the genomics community, FSR is arguably the most common method to perform multi-SNP analyses because of its intuitive simplicity (Stranger et al., 2012; Brown et al., 2013). The ARD prior also performs poorly. ARD has a fairly consistent precision—under 0.4—across a large range of recall values; this model does not have as much sparsity in the results as the other methods. Lasso performs better than FSR and ARD across all levels of recall. MAPS is a single point, because all PPI are either 0 or 1, so all thresholds between these points have the same PR; the recall is high, although the precision is lower than for BSR at that same level of recall. For biological feasibility, we consider the best comparison of the methods to be at a low FDR, as an FDR of 50% indicates that there are equal numbers of true positive and false positive biological hypotheses, decreasing their utility for expensive downstream analysis or experimental

validation.

Three observations about the relative performance of these methods highlight the promise of our Bayesian approach to structured sparsity. First, these simulations show the advantage of performing association testing on the posterior probability of inclusion rather than the absolute values of the regression coefficients themselves: all of our Bayesian sparse models perform better in the PR curves than any of the coefficient-based models (FSR, Lasso, ARD) at low FDR. The subtle but important distinction is that the coefficient-based models make the Zero Assumption (ZA) (Efron, 2008), which is that the z-scores of the estimated effect sizes near zero come from null associations, or, equivalently, that p-values near one represent null associations. Indeed, this is a central assumption in the q-value procedure to calculate FDR (Storey and Tibshirani, 2003). Practically, by selecting a global threshold for the β_j variables, all associations with effect sizes of smaller magnitude than the threshold are removed regardless of evidence for association.

PPI-based methods, however, do not make the ZA (Efron, 2008); in our two-groups model we have an explicit unimodal, zero-centered distribution on the effect size of the included predictors. Other dense-within-groups formulations have been proposed, including modeling the included predictors as a mixture of $K \ll p$ zero-mean Gaussians or uniform distributions with their start or end points at zero (Matthew Stephens, personal communication). We later suggest inducing sparse-within-groups behavior by modeling the variance of each of these Gaussian distributions separately. This is the benefit of using indicator variables in the global-local framework: each coefficient β_j is regularized globally (by parameter λ) but included or excluded locally (by coefficient-specific parameters γ_j), forcing weak signals to the null group, but rescuing low effect size predictors through structure. A drawback to our approach is that, for a similar FDR, the number of included variables in the model is typically much higher than for methods that make the ZA (Gelman et al., 2012).

Second, there is evidence that adding structure to the covariates improves the ability to perform association mapping: the precision recall curve for BSSR (structure) shows distinct improvement over BSR (no structure) except in a short region around 0.5 recall. Previous work (Guan and Stephens, 2011) has suggested that there is “no good reason to believe that the correlation structure of causal effects will follow that of the SNPs.” Our simulation results show that, while SNP correlation is a gross proxy for the correlation structure of independent causal effects, explicitly modeling SNP correlation does improve our ability to perform association mapping.

Third, model averaging appears to also confer an advantage over the MAP configuration, which we observe when comparing the PRCs of MAPS and BSSR results. It appears that model averaging protects against type I errors and the non-robust point estimates of MAP configurations, recapitulating previous work (Valdar et al., 2012; Wilson et al., 2010).

The comparative results for SimTag reflects qualitatively similar performance, although the scale of the precision is on half of the PRC figure for Sim1 (Figure 3). Interestingly, the performance of MAPS did not decrease proportionally as much as the other methods.

While precision-recall curves present aggregate results on these simulated data, it is also instructive to study results from individual simulations. We considered the results of six different methods applied to three simulated traits with 200 SNPs included in Sim1 (Figure 4). FSR appears to predict the truly alternative predictors well across the three examples, but the number of FP associations, and the substantial estimated effect size of those FP associations, hurt the precision of the results. Echoing PR curve findings, ARD results are dense, with many more non-zero effects relative to results from other methods. Lasso appears to have a high rate of false negatives, as reflected in its low sensitivity: Lasso finds no associations in the third example. Furthermore, for Lasso the FP predictors have estimates of the effect size equivalent to the effect size predicted for

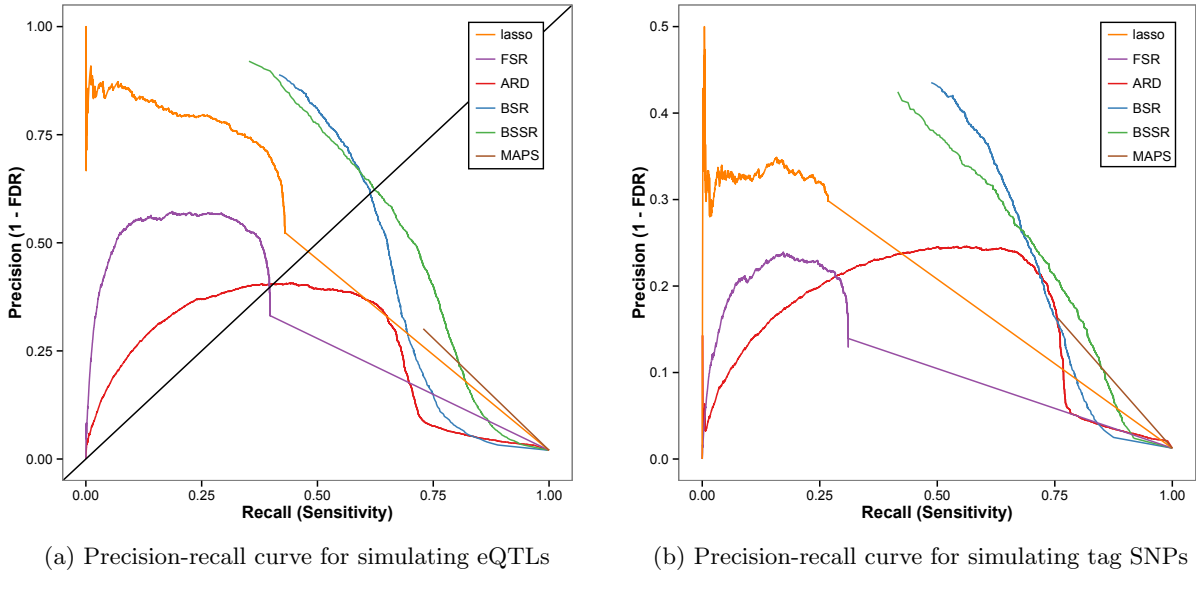


Fig 3: Precision-recall curves comparing five methods of association mapping using sparse regression methods on simulated data. Precision-recall curves comparing the different methods along recall (true positive rate; x-axis) versus precision ($1 - \text{FDR}$; y-axis). The legend shows which curves correspond to which method. **(A)** Precision-recall curves for Sim1. **(B)** Precision-recall curves for SimTag.

the TP predictors (e.g., first and second examples). BSR appears to identify the true positive values much of the time in these three examples, but appears to be confounded by correlation among the predictors, increasing the PPI of correlated predictors, but often not to the level of the true positives. BSSR has similar behavior because of its dense-within-groups behavior, and both show greater sensitivity than other methods in these examples: BSSR has two FNs with a conservative PPI threshold of 0.6, and BSR has three FNs. MAPS, the MAP configuration found during MCMC with BSSR estimates each predictor inclusion as either 0 or 1; as a result, there are more FPs than BSR and BSSR at similar sensitivity, but, in these examples, only three FNs.

5.2. Whole-genome *cis*-eQTLs. To validate that our Bayesian structured sparse regression model could be applied to whole-genome association mapping studies, we ran our method with the Σ^{cor} matrix on 16,242 genes with gene expression levels quantified using microarray data on the same 608 HapMap phase 3 individuals sampled from 14 distinct worldwide regions (Stranger et al., 2012). We compared the set of identified eQTLs in these data with the eQTLs we identified using a univariate analysis for Bayesian association mapping, SNPTEST (Marchini et al., 2007).

Studies of expression quantitative trait loci (eQTLs) often limit the number of tests for association by four orders of magnitude by restricting the set of SNPs tested for any gene to the SNPs in *cis* with that gene, or local to that gene. Many studies have suggested that, given our current limitations on sample size and the small effects of each eQTL on gene expression levels, we should restrict ourselves to identification of *cis*-eQTLs because local effects tend to be larger and there are many fewer tests, resulting in greater statistical power (Mangravite et al., 2013; Stranger et al., 2012, 2007; Morley et al., 2004). In this work, we restricted the SNPs tested for a given gene to those

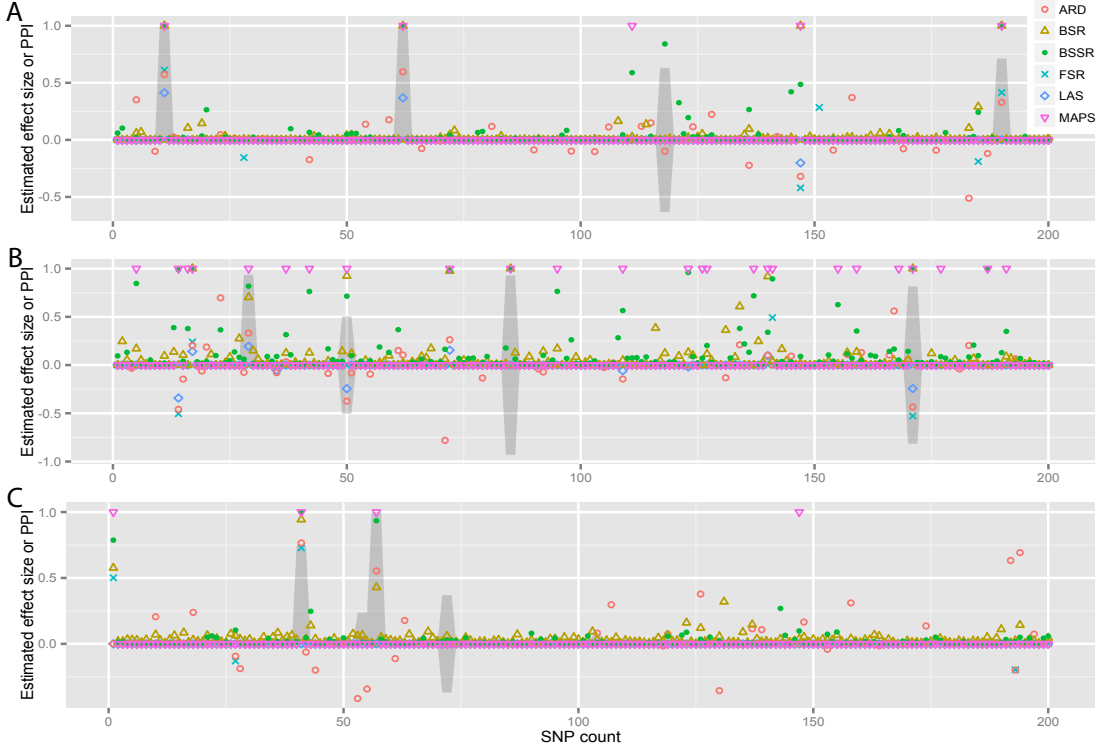


Fig 4: Three examples of results from six methods on simulated quantitative trait data. x-axis represents the SNP predictors, ordered along the chromosome; x-axis represents the estimated effect size (ARD, FSR, LAS) or the PPI (BSR, MAPS, BSSR). Truly alternative associations are shaded with the height of the shading representing their effect size; negative effect sizes are mirrored on the positive axis to highlight corresponding PPIs. Colors and shapes represent one of six methods shown in the legend; Red circles: Automatic relevance determination (ARD); Yellow triangles: Bayesian sparse regression (BSR); Green dots: Bayesian structured sparse regression (BSSR); Aqua X: Forward stepwise regression (FSR); Blue diamonds: Lasso regression (LAS); Pink triangles: MAP configuration for BSSR.

that are located within 200 Kb (or two hundred thousand bases) of the transcription start site (TSS) or transcription end site (TES) of a gene; thus, the size of the SNP window is 400 Kb plus the size of the gene. For each gene, there is an average of 6,152 cis-SNPs that were tested, for a total of 100,039,937 univariate gene-SNP tests.

We computed the FDR of a given threshold on the PPI from BSSR and on the \log_{10} Bayes factors (BF) from SNPTEST using a single complete permutation of the data. Specifically, we permuted the sample labels on the gene expression data matrix, and compute the inclusion probabilities and $\log_{10} BF$ s for every gene against every set of cis-SNPs, under the assumption that these BFs will represent the same number of tests under the null hypothesis of no association. Then, across possible inclusion probabilities and $\log_{10} BF$ thresholds, we computed FDR using the real and permuted

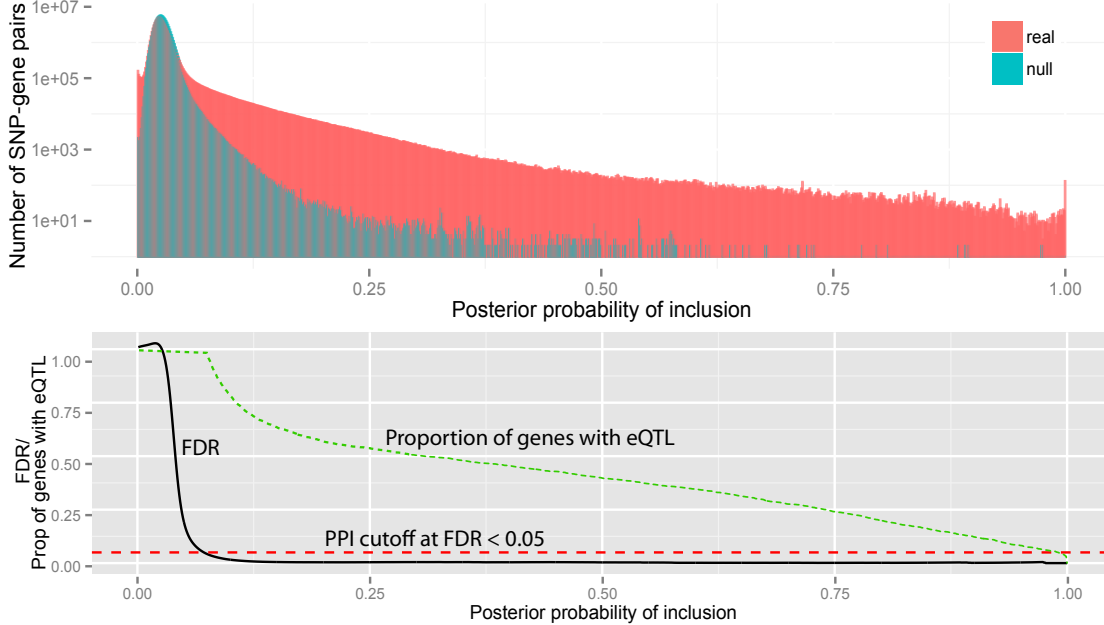


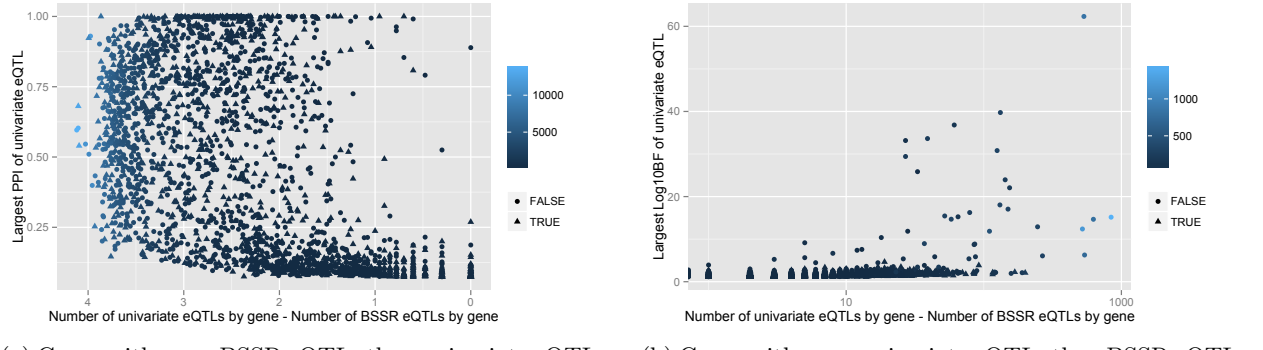
Fig 5: Application of BSSR to real and permuted data. The top histogram compares the number of SNP-gene pairs (y-axis; log₁₀ scale) at each PPI (x-axis) for an identical number of tests in the real data versus the permuted (null) data; the bottom figure shows the estimated FDR from these tests, with the red dashed line indicating an FDR = 0.05 and the green dotted line indicating the proportion of genes (out of the 2,589 total genes with eQTLs identified using BSSR) with one or more eQTLs at each PPI threshold.

results by:

$$\begin{aligned}\widehat{FDR}_{inc}(c_{ppi}) &= \frac{\sum_{g=1}^G \sum_{j=1}^p \mathbb{1}(p(\Gamma_{j,j,g}) > c_{ppi})}{\sum_{g=1}^G \sum_{j=1}^p \mathbb{1}(p(\Gamma_{j,j,g}^{perm}) > c_{ppi})} \\ \widehat{FDR}_{bf}(c_{bf}) &= \frac{\sum_{g=1}^G \sum_{j=1}^p \mathbb{1}(\log_{10} BF_{j,g} > c_{bf})}{\sum_{g=1}^G \sum_{j=1}^p \mathbb{1}(\log_{10} BF_{j,g}^{perm} > c_{bf})},\end{aligned}$$

where c_{ppi} and c_{bf} are the PPI threshold and the $\log_{10} BF$ threshold, respectively, and $p(\Gamma_{g,j,j})$, $\log_{10} BF_{g,j,j}$ are the PPIs and the $\log_{10} BF$ of the g^{th} gene and the j^{th} SNP, respectively, for $g = \{1, \dots, G\}$ genes. The superscript *perm* indicates that these metrics were evaluated on the permuted data. We compared the number of SNPs with $\log_{10} BF$ with the observed and permuted data and observed clear enrichment of large values (Figure 5A). We selected the PPI threshold to be $c_{ppi} = 0.072$ for $FDR \geq 5\%$.

We identified 2,940,533 cis-eQTLs using our multi-SNP association mapping ($FDR \leq 5\%$, $PPI \geq 0.073$), as compared to 169,460 cis-eQTLs found using the univariate association mapping method ($FDR \leq 5\%$, $\log_{10} BF \geq 1.092$). There were 2,589 out of 16,242 genes with at least one eQTL for BSSR versus 5,065 genes with at least one eQTL for the univariate association mapping method; of these, 1,463 genes had significant eQTLs for both approaches ($FDR \leq 5\%$). This order-of-magnitude increase in the number of cis-eQTLs is not unexpected given that our approach explicitly removes



(a) Genes with more BSSR eQTLs than univariate eQTLs (b) Genes with more univariate eQTLs than BSSR eQTLs

Fig 6: Comparison of eQTLs identified by univariate and BSSR approaches by gene. Each point represents a single gene for which at least one eQTL was identified using one of the two methods. X-axis (log₁₀ scale) is the difference in the number of eQTLs per gene by the univariate approach and the BSSR approach. Triangles represent genes for which the approach with fewer eQTLs identified zero eQTLs for that gene; circles represent genes for which the approach with fewer eQTLs identified at least one eQTL for that gene. **(A)** y-axis is the largest PPI for an eQTL within that gene. **(B)** y-axis is the largest log₁₀ BF for an eQTL within that gene.

the zero assumption ([Gelman et al., 2012](#)); but, accompanied with a decrease in the total number of genes with at least one eQTL, suggests that our method improves the precision of this approach when viewed in a gene-by-gene way ([Figure 5B](#)). These results suggest that the null hypothesis of no association may be incorrect in a multi-SNP setting: the PPI of a truly null predictor has less shrinkage toward zero when it is correlated with a truly alternative predictor, increasing the average PPI of the truly null predictors that are correlated with a truly alternative predictor. For genes with no causal SNPs, this null hypothesis was appropriate. We suggest presenting results for this model in rank order by gene to experimental biologists, indicating our confidence with the *cis*-eQTLs with largest PPIs for follow up experimental validation.

It is instructive to compare the results from BSSR to those from the univariate approach on a gene-by-gene basis. When we consider those genes for which the univariate approach found more eQTLs than the BSSR approach ([Figure 6](#), right hand side) we notice that, for all of the genes where BSSR identified zero eQTLs, the univariate approach did not find any eQTLs with a log₁₀ BF ≥ 5 , indicating possible false positives that are systematically eliminated using our model. In particular, there are 3,602 genes with zero BSSR-identified eQTLs, which only have a few univariate-derived eQTLs each, all with low log₁₀ BFs; these non-replicating associations across genes are candidates for false positive associations. Genes with univariate-derived eQTLs with the greatest statistical significance have at least one significant BSSR-derived eQTL; fewer BSSR-derived eQTLs for that gene may indicate weaker LD in this region. Conversely, we also considered the set of genes for which there were more BSSR-derived eQTLs than univariate-derived eQTLs ([Figure 6](#), left-hand side). While there are many fewer genes with zero univariate-derived eQTLs in this set (1,126 genes), these genes often include SNPs with large PPI. Echoing results from the simulations, this suggests that BSSR approaches are able to identify eQTLs with smaller effect sizes by exploiting small effect sizes across structured SNPs, resulting in high recall. On the other hand, there also appears to be inflation of eQTL signals in BSSR results, suggesting a sparse-within-groups model may have improved precision on a SNP-by-SNP basis.

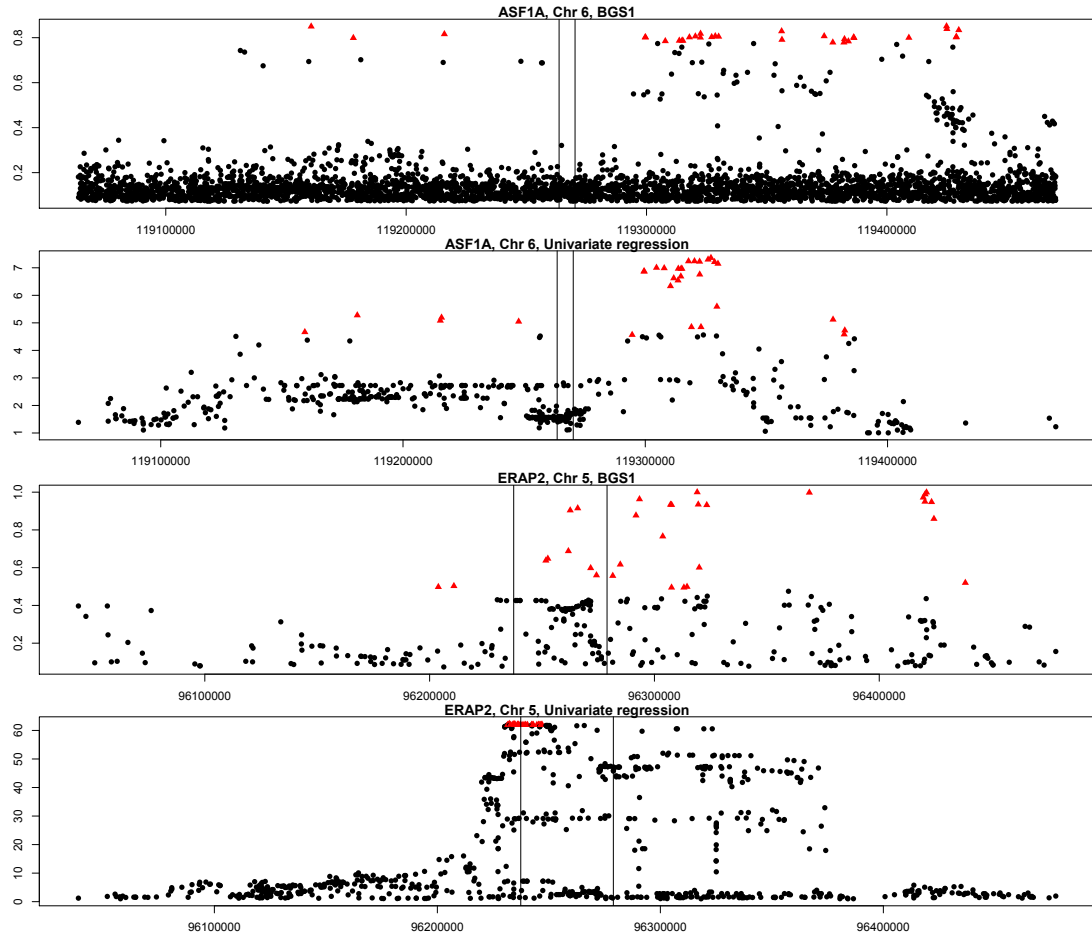


Fig 7: Results from BSSR and univariate approaches on two genes: ASF1A and ERAP2. The x-axis is the chromosomal position of each of the SNPs; the y-axis is the PPI (BSSR) or the $\log_{10} BF$ (univariate regression) of the SNP. Black circles represent statistically significant eQTLs ($FDR \leq 5\%$), red triangles represent the top 31 eQTLs for this gene from the two approaches. Horizontal lines denote the transcription start and end site of the gene.

We considered results from two specific genes (Figure 7). For *ASF1A*, we find that there are many more significant BSSR-identified eQTLs than univariate-identified eQTLs. We suspect that most of the eQTLs below 0.4 are included because they are well correlated with a causal SNP. In the case that the SNP is truly null, these eQTLs will be removed by a sparse-within-groups model; in the case that multiple causal SNPs are correlated, the sparse signal is effectively split between well correlated SNP, reducing the marginal PPIs. From the perspective of generating testable hypotheses, we highlight the 31 most significant SNPs, and find their range almost identical to the 31 most significant SNPs in the univariate regression analysis. Results from a second gene, *ERAP2*, show the opposite: the 31 most significant SNPs from the univariate analysis do not appear in the BSSR analysis, and the BSSR analysis highlights SNPs across a much larger range of the genome. On the far right, BSSR identifies clear signal that is poorly ranked in the univariate analysis because of small effect size. SNPs with similar PPI and $\log_{10} BF$ in both the BSSR and the univariate analysis (identifiable as lines of points looking vaguely horizontal) illustrate signal

splitting tendencies (in the case of BSSR) and the difficulties of finding the causal SNP amongst highly correlated predictors (in the case of the univariate analysis).

6. Discussion. In this manuscript, we introduced a general Bayesian structured sparse prior, encoding structure in the predictions via a Gaussian field, using an arbitrary positive definite matrix. We described its application in the context of regression to identify associations between genetic variants and quantitative traits where there is substantial structure in the genetic variants. We found that our prior robustly identifies directly associated predictors, and includes a natural statistical test for association. For recovering quantitative trait associations, we found many more associations per trait, but, across multivariate regression models, we found a smaller number of responses with one or more associated predictors across all tests.

In the original paper on group sparsity, the method encourages *dense within groups* sparsity, where either every member of the group was shrunk to zero or had minimal regularization (Yuan and Lin, 2005). However, there are good arguments in favor of *sparse within groups* sparsity, which shrinks groups to zero together, but also encourages individual sparsity (Friedman et al., 2010). In practice this decision is tailored to the application and the interpretation of the variables. The latter is certainly more natural in the framework of correlated coefficients, because we would like to select the smallest number of covariates that explain the variation in the data rather than a dense set with redundancies. However, from the Bayesian perspective, the sparse-within-groups model does not have a posterior mode that is robust to sample bias, and, instead, Bayesian statisticians find the dense-within-groups model more interpretable and generalizable (Valdar et al., 2012). Our formulation of Bayesian structured sparsity is dense-within-groups; however there are straightforward ways to tailor the model to achieve explicit sparse-within-groups performance, in particular, to modify the scalar global regularization term λ to be local p -vector predictor specific regularization. Because we are working within a multivariate regression framework, if two predictors have a similar effect on the response, the model will tend to select one for inclusion, and the posterior probability of inclusion for the two predictors will split the effect. This is where model averaging is helpful in encouraging the choice of included predictors to be robust.

A number of other extensions are interesting to consider in light of the application of these models to high-dimensional data. First, while our sampler is efficient and produces an estimate of the marginal PPI for each predictor, we would like to scale this to perform analytical association mapping for genome-scale data sets, which currently include approximately 40 million SNPs and thousands or tens of thousands of individuals (Jallow et al., 2009). One option is to window the entire genome into blocks of 10,000 SNPs, and perform association mapping within each of these windows in parallel. While this is easy to do, it is somewhat unsatisfying. It is desirable to consider other approaches, including multiscale methods and robust adaptations of stochastic variational methods for $p \gg n$ applications. Second, the additive assumptions implicit in this model are, with a few exceptions, made across this field of research (Storey et al., 2005), but ideally we would identify epistatic effects, or non-additive interacting effects, between predictors.

While we have presented this structured sparse framework based on GP probit regression, there are a large number of alternatives to this specific choice of prior that may be explored while maintaining tractability and expressiveness of this framework.

7. Conclusions. We present a general formulation for Bayesian structured sparsity that includes information about covariate structure in a positive definite matrix. Shrinkage is shared across inclusion variables for similar covariates via a Gaussian field. Applying this approach to regression models for association mapping for quantitative traits, we find that this method has a number of

statistical and computational advantages over current approaches. Furthermore, the arbitrary positive definite matrix allows the model to be tailored to arbitrary applications using domain-specific measures of similarity between predictors and that the pairwise similarity may be arbitrarily complex. Computationally, these methods are tractable for large studies and will be useful for many applications of structured sparsity and model selection. Accompanying Python code is available at <https://github.com/HIPS/BayesianStructuredSparsity>.

Acknowledgements. BEE was funded by BEE was funded through NIH NHGRI R00-HG006265 and NIH NIMH R01-MH101822. RPA was partially funded by DARPA Young Faculty Award N66001-12-1-4219.

References.

- James H. Albert and Siddhartha Chib. Bayesian analysis of binary and polychotomous response data. *Journal of the American Statistical Association*, 88(422):669–679, 1993.
- Artin Armagan, David Dunson, and Jaeyong Lee. Generalized double Pareto shrinkage. *preprint arXiv:1104.0861*, 2011a.
- Artin Armagan, DB Dunson, and Merlise Clyde. Generalized beta mixtures of Gaussians. *arXiv preprint arXiv:1107.4976*, pages 1–9, 2011b.
- Anirban Bhattacharya, Debdeep Pati, Natesh S. Pillai, and David B. Dunson. Bayesian shrinkage. December 2012.
- C. I. Bliss. The calculation of the dosage-mortality curve. *Annals of Applied Biology*, 22(1):134–167, February 1935.
- Leonardo Bottolo, Enrico Petretto, Stefan Blankenberg, François Cambien, Stuart a Cook, Laurence Tiret, and Sylvia Richardson. Bayesian detection of expression quantitative trait loci hot spots. *Genetics*, 189(4):1449–59, December 2011.
- Leo Breiman. Statistical modeling: The two cultures. *Statistical Science*, 16(3):199–231, 2001.
- Christopher D. Brown, Lara M. Mangravite, and Barbara E. Engelhardt. Integrative Modeling of eQTLs and Cis-Regulatory Elements Suggests Mechanisms Underlying Cell Type Specificity of eQTLs. *PLoS Genetics*, 9(8), August 2013.
- P. J. Brown, M. Vannucci, and T. Fearn. Bayes model averaging with selection of regressors. *Journal of the Royal Statistical Society: Series B (Statistical Methodology)*, 64(3):519–536, August 2002.
- Carlos M. Carvalho, Nicholas G. Polson, and James G. Scott. Handling sparsity via the horseshoe. *Journal of Machine Learning Research: Workshop and Conference Proceedings*, 5:73–80, 2009.
- Carlos M. Carvalho, Nicholas G. Polson, and James G. Scott. The horseshoe estimator for sparse signals. *Biometrika*, 97(2):465–480, 2010.
- Xi Chen, Qihang Lin, Seyoung Kim, Jaime G. Carbonell, and Eric P. Xing. Smoothing proximal gradient method for general structured sparse regression. *The Annals of Applied Statistics*, 6(2):719–752, June 2012.
- International HapMap Consortium et al. A haplotype map of the human genome. *Nature*, 437(7063):1299–1320, 2005.
- International HapMap 3 Consortium et al. Integrating common and rare genetic variation in diverse human populations. *Nature*, 467(7311):52–58, 2010.
- Richard M. Durbin, David L. Altshuler, and Gonçalo R. et al. Abecasis. A map of human genome variation from population-scale sequencing. *Nature*, 467(7319):1061–1073, October 2010.
- Bradley Efron. Microarrays, Empirical Bayes and the Two-Groups Model. *Statistical Science*, 23(1):1–22, March 2008.
- Bradley Efron and Trevor Hastie. Least angle regression. *The Annals of Statistics*, pages 1–44, 2004.
- Adi Fledel-Alon, Ellen Miranda Leffler, Yongtao Guan, Matthew Stephens, Graham Coop, and Molly Przeworski. Variation in human recombination rates and its genetic determinants. *PloS One*, 6(6):e20321, January 2011.
- Jerome Friedman, Trevor Hastie, and Robert Tibshirani. A note on the group lasso and a sparse group lasso. *arXiv preprint arXiv:1001.0736*, 2010.
- Stacey B Gabriel, Stephen F Schaffner, Huy Nguyen, Jamie M Moore, Jessica Roy, Brendan Blumenstiel, John Higgins, Matthew DeFelice, Amy Lochner, Maura Faggart, et al. The structure of haplotype blocks in the human genome. *Science*, 296(5576):2225–2229, 2002.
- Andrew Gelman, Jennifer Hill, and Masanao Yajima. Why we (usually) don’t have to worry about multiple comparisons. *Journal of Research on Educational Effectiveness*, 5(2):189–211, 2012.
- EI George and RE McCulloch. Variable selection via Gibbs sampling. *Journal of the American Statistical Association*, 88(423):881–889, 1993.

- Mark Girolami and Simon Rogers. Variational Bayesian Multinomial Probit Regression with Gaussian Process Priors. *Neural Computation*, 18(8):1790–1817, August 2006.
- Yongtao Guan and Matthew Stephens. Bayesian variable selection regression for genome-wide association studies and other large-scale problems. *The Annals of Applied Statistics*, 5(3):1780–1815, September 2011.
- Chris Hans. Bayesian lasso regression. *Biometrika*, 96(September):835–845, 2009.
- Clive J Hoggart, John C Whittaker, Maria De Iorio, and David J Balding. Simultaneous analysis of all SNPs in genome-wide and re-sequencing association studies. *PLoS Genetics*, 4(7), January 2008.
- Hemant Ishwaran and J. Sunil Rao. Spike and slab variable selection: Frequentist and Bayesian strategies. *The Annals of Statistics*, 33(2):730–773, April 2005.
- Laurent Jacob, G Obozinski, and JP Vert. Group lasso with overlap and graph lasso. *Proceedings of the 26th International Conference on Machine Learning*, 2009.
- Muminatou Jallow, Yik Ying Teo, and et al. Genome-wide and fine-resolution association analysis of malaria in West Africa. *Nature Genetics*, 41(6):657–65, June 2009.
- Sir Harold Jeffreys. *The Theory of Probability*, volume 9. Oxford University Press, Oxford, England, 1998.
- Rodolphe Jenatton, JY Audibert, and Francis Bach. Structured variable selection with sparsity-inducing norms. *The Journal of Machine Learning Research*, 2011a.
- Rodolphe Jenatton, J Mairal, Guillaume Obozinski, and Francis Bach. Proximal methods for hierarchical sparse coding. *The Journal of Machine Learning Research*, 12:2297–2334, 2011b.
- C M Kendziora, M Chen, M Yuan, H Lan, and a D Attie. Statistical methods for expression quantitative trait loci (eQTL) mapping. *Biometrics*, 62(1):19–27, March 2006.
- Seyoung Kim. Tree-guided group lasso for multi-task regression with structured sparsity. *Arxiv preprint arXiv:0909.1373*, 2009.
- Seyoung Kim and Eric P Xing. Statistical estimation of correlated genome associations to a quantitative trait network. *PLoS Genetics*, 5(8), August 2009.
- J. Z. Kolter, Siddharth Batra, and Andrew Y. Ng. Energy disaggregation via discriminative sparse coding. In J.D. Lafferty, C.K.I. Williams, J. Shawe-Taylor, R.S. Zemel, and A. Culotta, editors, *Advances in Neural Information Processing Systems 23*, pages 1153–1161, 2010.
- Minjung Kyung, Jeff Gill, Malay Ghosh, and George Casella. Penalized regression, standard errors, and Bayesian lassos. *Bayesian Analysis*, 5(2):369–412, 2010.
- Hana Lango Allen, Karol Estrada, and Guillaume et al. Lettre. Hundreds of variants clustered in genomic loci and biological pathways affect human height. *Nature*, 467(7317):832–8, October 2010.
- Han Liu, John Lafferty, and Larry Wasserman. Nonparametric Regression and Classification with Joint Sparsity Constraints Joint Sparsity Constraints. *Computer Science Department, Paper 1034*, 2008.
- Lara M. Mangravite, Barbara E. Engelhardt, Marisa W. Medina, Joshua D. Smith, Christopher D. Brown, Daniel I. Chasman, Brigham H. Mechem, Bryan Howie, Heejung Shim, Devesh Naidoo, QiPing Feng, Mark J. Rieder, Yii-Der I. Chen, Jerome I. Rotter, Paul M. Ridker, Jemma C. Hopewell, Sarah Parish, Jane Armitage, Rory Collins, Russell A. Wilke, Deborah A. Nickerson, Matthew Stephens, and Ronald M. Krauss. A statin-dependent QTL for GATM expression is associated with statin-induced myopathy. *Nature*, August 2013.
- Joseph C Maranville, Francesca Luca, Allison L Richards, Xiaoquan Wen, David B Witonsky, Shannen Baxter, Matthew Stephens, and Anna Di Rienzo. Interactions between glucocorticoid treatment and cis-regulatory polymorphisms contribute to cellular response phenotypes. *PLOS Genetics*, 7(7), 2011.
- Jonathan Marchini, Bryan Howie, Simon Myers, Gil McVean, and Peter Donnelly. A new multipoint method for genome-wide association studies by imputation of genotypes. *Nature Genetics*, 39(7):906–13, July 2007.
- Nicolai Meinshausen and B Peter. Stability selection. *Journal of the Royal Statistical Society*, pages 1–30, 2010.
- T. J. Mitchell and J. J. Beauchamp. Bayesian Variable Selection in Linear Regression. *Journal of the American Statistical Association*, 83(404):1023–1032, 1988.
- Shakir Mohamed, Katherine Heller, and Zoubin Ghahramani. Bayesian and l_1 approaches to sparse unsupervised learning. *arXiv preprint arXiv:1106.1157*, 2011.
- M Morley, C M Molony, T M Weber, J L Devlin, K G Ewens, R S Spielman, and V G Cheung. Genetic analysis of genome-wide variation in human gene expression. *Nature*, 430(7001), 2004.
- Iain Murray, Ryan P. Adams, and David J. C. MacKay. Elliptical slice sampling. In *Proceedings of the 13th International Conference on Artificial Intelligence and Statistics*, pages 541–548, 2010.
- Radford M. Neal. Slice sampling. *The Annals of Statistics*, 31(3):705–767, 2003.
- R. B. O’Hara and M. J. Sillanpää. A review of Bayesian variable selection methods: what, how and which. *Bayesian Analysis*, 4(1):85–117, March 2009.
- Enrico Petretto, Leonardo Bottolo, Sarah R Langley, Matthias Heinig, Chris McDermott-Roe, Rizwan Sarwar, Michal Pravenec, Norbert Hübner, Timothy J Aitman, Stuart A Cook, and Sylvia Richardson. New insights into the genetic

- control of gene expression using a Bayesian multi-tissue approach. *PLoS Computational Biology*, 6(4), April 2010.
- Nicholas G. Polson and James G. Scott. Shrink globally, act locally: sparse Bayesian regularization and prediction. *Bayesian Statistics*, 2010.
- Matthew D Rasmussen, Melissa J Hubisz, Ilan Gronau, and Adam Siepel. Genome-wide inference of ancestral recombination graphs. *PLoS genetics*, 10(5):e1004342, 2014.
- S Richardson, Leonardo Bottolo, and JS Rosenthal. Bayesian models for sparse regression analysis of high dimensional data. *Bayesian Statistics*, 2010.
- G Schwarz. Estimating the Dimension of a Model. *The Annals of Statistics*, 6(6):461–464, 1978.
- Matthias Seeger. Covariance kernels from Bayesian Generative Models. *Advances in Neural Information Processing Systems 14*, 2000.
- Michael Smith and Robert Kohn. Nonparametric regression using Bayesian variable selection. *Journal of Econometrics*, 1996.
- Matthew Stephens and David J Balding. Bayesian statistical methods for genetic association studies. *Nature Reviews Genetics*, 10(10):681–90, October 2009.
- John D Storey and Robert Tibshirani. Statistical significance for genomewide studies. *Proceedings of the National Academy of Sciences of the United States of America*, 100(16):9440–5, August 2003.
- John D Storey, Joshua M Akey, and Leonid Kruglyak. Multiple locus linkage analysis of genomewide expression in yeast. *PLoS biology*, 3(8):e267, August 2005.
- Barbara E Stranger, Alexandra C Nica, Matthew S Forrest, Antigone Dimas, Christine P Bird, Claude Beazley, Catherine E Ingle, Mark Dunning, Paul Flück, Daphne Koller, Stephen Montgomery, Simon Tavaré, Panos Deloukas, and Emmanouil T Dermitzakis. Population genomics of human gene expression. *Nature Genetics*, 39(10):1217–1224, October 2007.
- Barbara E. Stranger, Stephen B. Montgomery, Antigone S. Dimas, Leopold Parts, Oliver Stegle, Catherine E. Ingle, Magda Sekowska, George Davey Smith, David Evans, Maria Gutierrez-Arcelus, Alkes Price, Towfique Raj, James Nisbett, Alexandra C. Nica, Claude Beazley, Richard Durbin, Panos Deloukas, and Emmanouil T. Dermitzakis. Patterns of Cis Regulatory Variation in Diverse Human Populations. *PLOS Genetics*, 8(4), April 2012.
- R Tibshirani. Regression shrinkage and selection via the LASSO. *Journal of the Royal Statistical Society: Series B*, 58(1):267—288, 1996.
- Robert J Tibshirani. In praise of sparsity and convexity. *Past, Present, and Future of Statistical Science*, page 495, 2014.
- M E Tipping. Sparse Bayesian learning and the relevance vector machine. *Journal of Machine Learning Research*, 1:211–244, 2001.
- Joel A Tropp and Stephen J Wright. Computational methods for sparse solution of linear inverse problems. *Proceedings of the IEEE*, 98(6):948–958, 2010.
- William Valdar, Jeremy Sabourin, Andrew Nobel, and Christopher C. Holmes. Reprioritizing Genetic Associations in Hit Regions Using LASSO-Based Resample Model Averaging. *Genetic Epidemiology*, 12, April 2012.
- Melanie A. Wilson, Edwin S. Iversen, Merlise A. Clyde, Scott C. Schmidler, and Joellen M. Schildkraut. Bayesian model search and multilevel inference for SNP association studies. *The Annals of Applied Statistics*, 4(3):1342–1364, September 2010.
- Andrew R Wood, Dena G Hernandez, Michael a Nalls, Hanieh Yaghootkar, J Raphael Gibbs, Lorna W Harries, Sean Chong, Matthew Moore, Michael N Weedon, Jack M Guralnik, Stefania Bandinelli, Anna Murray, Luigi Ferrucci, Andrew B Singleton, David Melzer, and Timothy M Frayling. Allelic heterogeneity and more detailed analyses of known loci explain additional phenotypic variation and reveal complex patterns of association. *Human Molecular Genetics*, 20(20):4082–92, October 2011.
- Tong Tong Wu, Yi Fang Chen, Trevor Hastie, Eric Sobel, and Kenneth Lange. Genome-wide association analysis by lasso penalized logistic regression. *Bioinformatics (Oxford, England)*, 25(6):714–21, March 2009.
- Jian Yang, Beben Benyamin, Brian P McEvoy, Scott Gordon, Anjali K Henders, Dale R Nyholt, Pamela A Madden, Andrew C Heath, Nicholas G Martin, Grant W Montgomery, Michael E Goddard, and Peter M Visscher. Common SNPs explain a large proportion of the heritability for human height. *Nature genetics*, 42(7):565–9, July 2010.
- Jian Yang, Teresa Ferreira, Andrew P Morris, Sarah E Medland, Pamela A F Madden, Andrew C Heath, Nicholas G Martin, Grant W Montgomery, Michael N Weedon, Ruth J Loos, Timothy M Frayling, Mark I McCarthy, Joel N Hirschhorn, Michael E Goddard, and Peter M Visscher. Conditional and joint multiple-SNP analysis of GWAS summary statistics identifies additional variants influencing complex traits. *Nature Genetics*, 44(4):369–75, S1–3, April 2012.
- M. Yuan and Y. Lin. Model selection and estimation in regression with grouped variables. *Journal of the Royal Statistical Society: Series B*, 68(1):49–67, 2005.
- Hui Zou and Trevor Hastie. Regularization and variable selection via the elastic net. *Journal of the Royal Statistical*

Society: Series B (Statistical Methodology), 67(2):301–320, 2005.

BARBARA E. ENGELHARDT
DEPARTMENT OF BIOSTATISTICS & BIOINFORMATICS
INSTITUTE FOR GENOMIC SCIENCE & POLICY
DEPARTMENT OF STATISTICAL SCIENCE
DUKE UNIVERSITY
DURHAM, NC
E-MAIL: barbara.engelhardt@duke.edu

RYAN P. ADAMS
SCHOOL OF ENGINEERING AND APPLIED SCIENCES
HARVARD UNIVERSITY
CAMBRIDGE, MA
E-MAIL: rpa@seas.harvard.edu